Research Square

Preprints are preliminary reports that have not undergone peer review.
They should not be considered conclusive, used to inform clinical practice,
or referenced by the media as validated information.

From Suitability Mapping to Resilient Cultivation Planning: A Geospatial Framework for Identifying Climate-Stable Refugia

Tuan A. Pham
Tay Bac University
Tuan A. Pham
atpham@kth.se

KTH Royal Institute of Technology

Article

Keywords: Panax notoginseng, climate-stable cultivation refugia, climate-model uncertainty, CMIP6, GIS–Fuzzy-AHP, land-use feasibility

Posted Date: October 26th, 2026

DOI: https://doi.org/10.21203/rs.3.rs-10114377/v1

License: This work is licensed under a Creative Commons Attribution 4.0 International License.
Read Full License

Additional Declarations: No competing interests reported.

An Uncertainty-Aware Geospatial Framework for Climate-Resilient Cultivation Planning of *Panax notoginseng* in Northern Vietnam

Tuan A. Pham[1], Tuan A. Pham[2,3*]

[1]*Faculty of Social Sciences, Tay Bac University, Son La, Vietnam*

ORCID: 0000-0003-3986-647X

Email: phamtuan@utb.edu.vn

[2]*Department of Civil and Architectural Engineering, KTH Royal Institute of Technology, Stockholm, SE-100 44, Sweden*

[3]*Smart Computing in Civil Engineering Research Group, Faculty of Civil Engineering, Ton Duc Thang University, Ho Chi Minh City, Vietnam*

Corresponding email: atpham@kth.se; phamanhtuan@tdtu.edu.vn;

ORCID: 0000-0002-9937-3442

**Corresponding author: Tuan A. Pham*

Abstract

High-value medicinal plants with narrow ecological tolerances are increasingly threatened by climate change, yet cultivation planning often overlooks climate-model uncertainty and land-use constraints. We developed an uncertainty-aware geospatial framework to support climate-resilient cultivation planning for *Panax notoginseng* in northern Vietnam. The framework integrates GIS-based Fuzzy Analytic Hierarchy Process (Fuzzy-AHP) modelling, non-compensatory ecological thresholds, five CMIP6 climate models, two high-emission scenarios (SSP3-7.0 and SSP5-8.5), model–scenario consensus analysis, and land-use exclusion masks. The baseline suitability model, independently evaluated using 27 published occurrence records, achieved an AUC of 0.68 and a continuous Boyce index of 0.93. Under baseline conditions, highly suitable land covered approximately 7,250 km² (7.9% of the valid study area). By 2041–2070, the ensemble-mean highly suitable area decreased to approximately 2,330 km² under SSP3-7.0 and 1,580 km² under SSP5-8.5, representing reductions of 68% and 78%, respectively. Although individual projections identified broader suitable areas, high-confidence climate-stable S1 cores were much smaller, declining from 3,830 km² at the weakest agreement threshold to 139 km² under full agreement. Increasingly stringent model–scenario agreement was the main driver of the reduction in candidate land; after land-use exclusions, potentially available cultivation land ranged from 3,360 km² to 127 km² across consensus thresholds, and most excluded stable-core land was conservation-designated. The framework provides uncertainty-aware decision-support maps for climate-smart cultivation and conservation planning, while recognizing that field validation, tenure, accessibility, and socioeconomic feasibility remain necessary before site-level implementation.

Keywords*:* *Panax notoginseng; climate-stable cultivation refugia; climate-model uncertainty; CMIP6; GIS–Fuzzy-AHP; land-use feasibility*.

INTRODUCTION

Medicinal plants provide essential ecosystem services, support rural livelihoods, and constitute a critical source of bioactive compounds for pharmaceutical development. Among these species, Panax notoginseng (Burk.) F.H. Chen is one of the most valuable medicinal herbs in East Asia, widely recognized for its anti-inflammatory, antioxidant, cardiovascular, neuroprotective, anticancer, and immunomodulatory properties [1–3]. Its roots contain high concentrations of ginsenosides and other pharmacologically active compounds that underpin its extensive use in traditional and modern medicine [4]. In Vietnam, P. notoginseng is considered a strategic medicinal resource and is prioritized for germplasm conservation and cultivation development under national medicinal plant programs [1,5].

Despite its high economic and medicinal value, *P. notoginseng* exhibits exceptionally narrow ecological requirements. The species is adapted to cool and humid mountain environments and is highly sensitive to changes in temperature, precipitation, elevation, and soil conditions. Consequently, its cultivation is largely restricted to high-altitude regions of southwestern China and northern Vietnam [1,5]. Such ecological specialization makes the species particularly vulnerable to climate change. Increasing temperatures, altered precipitation regimes, and shifting suitable climatic niches are expected to change the geographic distribution of many mountain species worldwide, with medicinal plants among the most vulnerable due to their often-restricted ranges and limited adaptive capacity. Recent studies have projected substantial habitat contraction and upslope migration for numerous climate-sensitive medicinal species, raising concerns about the sustainability of future cultivation, biodiversity conservation, and the security of medicinal resources.

Identifying areas that remain suitable under future climate conditions is therefore becoming an essential component of climate-smart agricultural planning [6,7]. However, suitability alone does not necessarily imply long-term cultivation viability [8–10]. Areas projected to be suitable by a single climate model may become unsuitable under alternative climate projections, while many environmentally suitable locations may be inaccessible due to land-use conflicts, protected-area regulations, or physical constraints. Consequently, sustainable cultivation planning requires a more comprehensive perspective that integrates ecological suitability, climate uncertainty, and land-use feasibility within a unified decision-support framework.

Species distribution studies have traditionally relied on two broad methodological approaches. Correlative ecological niche models, such as Maximum Entropy (MaxEnt), infer species–environment relationships from occurrence records and are widely used for projecting future habitat distributions. Although powerful, these approaches often require extensive occurrence datasets and may be sensitive to sampling bias and model assumptions. Alternatively, knowledge-based approaches combine Geographic Information Systems (GIS) with Multi-Criteria Decision Analysis (MCDA), deriving environmental suitability from ecological knowledge and expert judgment [11–13]. Among these methods, the Fuzzy Analytic Hierarchy Process (Fuzzy-AHP) has emerged as a particularly attractive framework because it incorporates uncertainty in expert assessments while maintaining transparency and interpretability for practical decision-making [14]. Nevertheless, most existing GIS-based suitability studies focus primarily on identifying suitable areas under current or future conditions and rarely distinguish between transient suitability and climate-stable cultivation zones [15,16]. The two families are complementary: correlative models infer species–environment relationships from occurrence records, whereas knowledge-based models explicitly encode published physiological thresholds, and both have been applied to the genus in southwestern China and the eastern Himalaya. The present study follows the knowledge-based route and therefore treats occurrence records as an independent evaluation set rather than as calibration data.

A second limitation concerns how we treat climate uncertainty. Future suitability projections are commonly represented by ensemble means, which can obscure substantial disagreement among climate models and emission scenarios. For decision-makers, understanding where multiple projections consistently identify suitable conditions may be more valuable than relying solely on average projections. Such areas can be considered candidate locations for climate refugia, where favorable environmental conditions are likely to persist despite climate change. Identifying these refugia is increasingly recognized as a key strategy for biodiversity conservation and climate adaptation, yet it remains underexplored in the planning of medicinal plant cultivation.

A third limitation is that ecological suitability assessments seldom incorporate practical land availability. Conservation areas, national parks, settlements, transportation corridors, wetlands, and other land-use constraints can substantially reduce the area that is realistically available for cultivation. As a result, suitability maps may significantly overestimate future cultivation opportunities if they do not explicitly account for feasibility considerations.

To address these gaps, this study develops an uncertainty-aware geospatial framework for climate-resilient cultivation planning of *Panax notoginseng* in the mountainous regions of northern Vietnam. The framework integrates GIS-based Fuzzy Analytic Hierarchy Process (Fuzzy-AHP) modelling, non-compensatory ecological constraints, CMIP6 climate projections, per-cell model–scenario consensus analysis, and spatial land-use exclusion masks. It distinguishes among: (i) present and future ecological suitability, (ii) climate-stable highly suitable areas supported across alternative climate projections, (iii) potential migration zones, and (iv) land-use-feasible cultivation zones.

In this study, "climate-stable cultivation refugia" refers operationally to areas classified as highly suitable under baseline conditions and retained as highly suitable under at least 8 of 10 future GCM–scenario projections. The term denotes model-based decision-support zones, rather than empirically verified demographic refugia. We test three hypotheses: (1) climate warming will substantially reduce the area classified as highly suitable for cultivation; (2) areas that remain highly suitable across multiple climate models and emission scenarios will constitute only a small fraction of the total area projected as suitable; and (3) physical and conservation-related land-use constraints will further reduce the land available for cultivation.

By integrating ecological suitability, climate stability, and land-use feasibility, the framework moves beyond conventional suitability mapping toward spatially explicit cultivation prioritization under climate uncertainty (Figure 1). The workflow may be transferable to other climate-sensitive medicinal plants and mountain crops, but its implementation requires local recalibration and independent validation. Specifically, the environmental thresholds, Fuzzy-AHP weights, ecological veto criteria, suitability-class breakpoints, and land-use exclusion rules are species- and jurisdiction-specific and must be re-derived using locally relevant ecological evidence, climatic data, land-use conditions, and legal frameworks before application elsewhere.

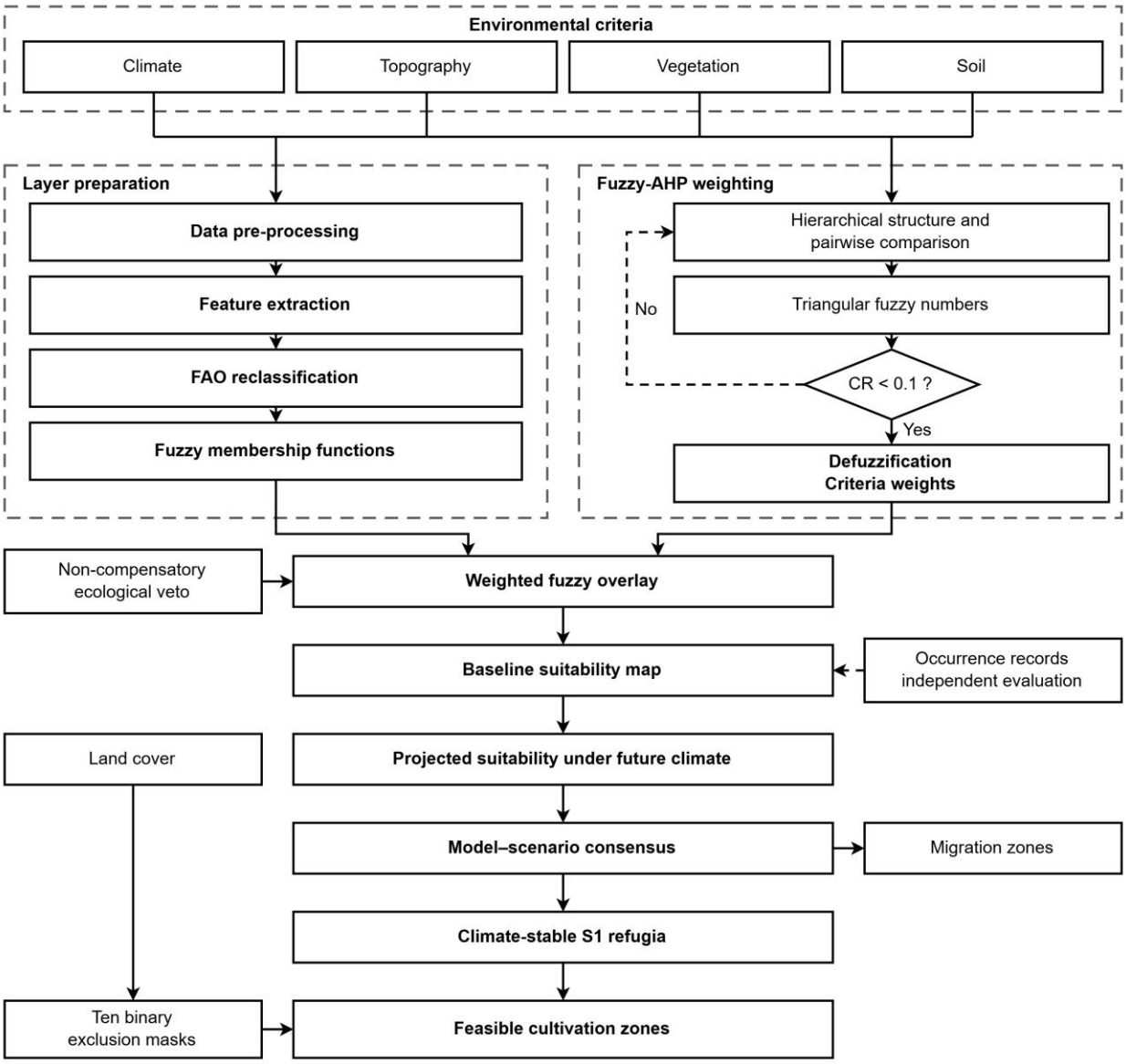


Figure 1. Analytical workflow for identifying climate-stable and land-use-feasible cultivation zones for Panax notoginseng under climate change. Input datasets and their native resolutions are given in Supplementary Table S2, and the provenance of the occurrence records is given in Supplementary Table S15. The land-cover layer is not a suitability criterion: it enters the workflow as the ten binary exclusion masks applied at the final step. The occurrence records are used only to evaluate the baseline surface; they do not enter the weighting, membership functions, or overlay. The authors drew the diagram; the editable source file is supplied with this revision.

METHODS

Study area

The study was conducted in the northern mountainous region of Vietnam, the principal ecological zone for *Panax notoginseng* cultivation in the country. The region comprises nine provinces with complex

topography, steep elevational gradients, and diverse climatic conditions. Elevation ranges from lowland valleys to mountain peaks exceeding 3,000 m above sea level, creating pronounced variations in temperature, precipitation, and soil development. These environmental gradients make the region particularly suitable for evaluating the ecological requirements and climate sensitivity of mountain medicinal plants. All spatial analyses were performed on a common 30-m computational grid in the WGS 84 / UTM Zone 48N coordinate system (EPSG:32648), shown in Figure 2. We distinguish throughout between this computational grid size (30 m), the native resolution of each input layer (Supplementary Table S2), and the effective information resolution, set by the coarsest contributing layer: approximately 1 km for the climatic predictors and 250 m for the soil predictors.

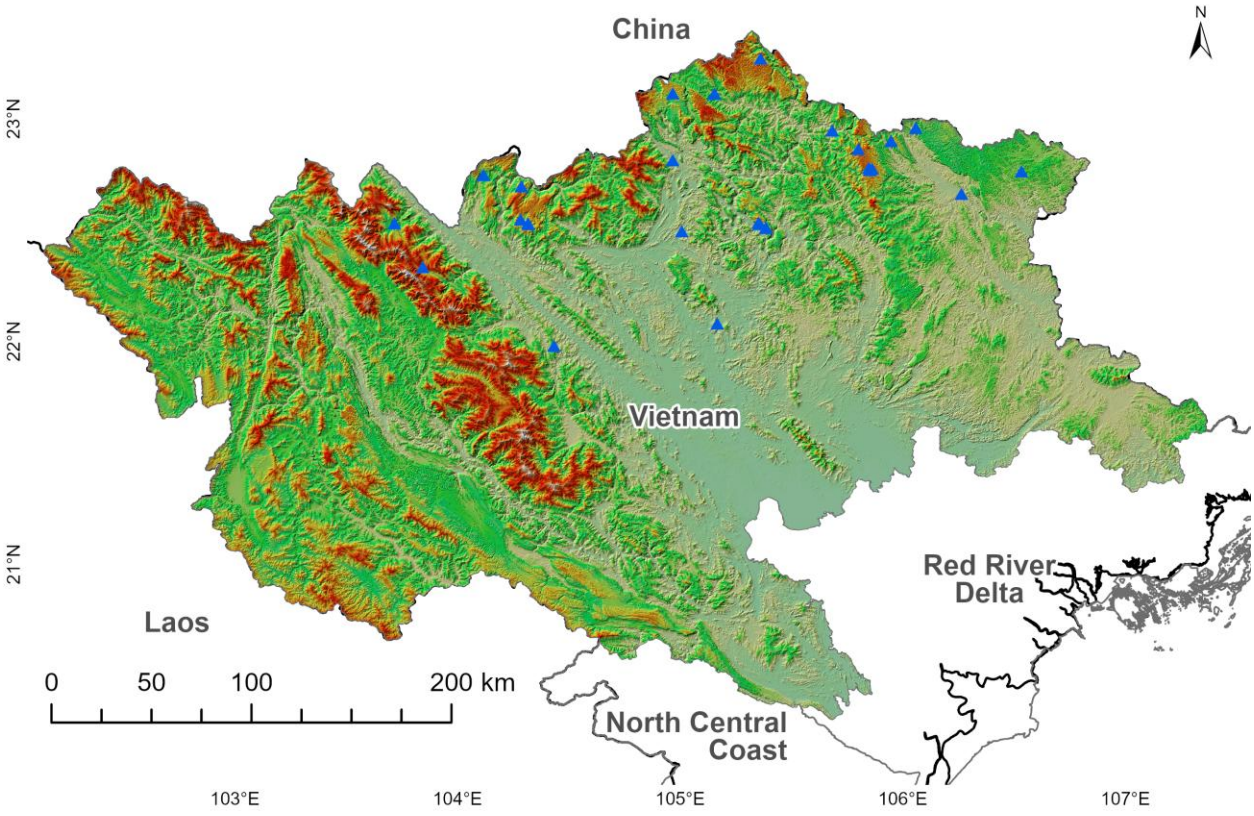


Figure 2. Study area in the northern mountainous region of Vietnam, showing the 27 published occurrence records of Panax notoginseng used to independently evaluate the baseline suitability surface. The authors created the maps in ArcGIS Pro 3.7 (Esri; https://www.esri.com/en-us/arcgis/products/arcgis-pro/).

Environmental data and land-use constraints

We evaluated ecological suitability using fifteen environmental criteria representing climatic, topographic, vegetation, and soil conditions (Supplementary Table S1). Climatic predictors included mean annual temperature (MAT), maximum temperature of the warmest month (T_{max}), minimum temperature of the coldest month (T_{min}), annual precipitation (AP), and precipitation of the coldest quarter (PCQ). Baseline climatic conditions (1981–2010) were obtained from CHELSA v2.1 [17].

Topographic predictors included elevation, slope, aspect, and topographic wetness index (TWI), derived from the 30-m Shuttle Radar Topography Mission (SRTM) digital elevation model [18]. Vegetation

conditions were represented by the normalized difference vegetation index (NDVI), calculated from Landsat 8 and 9 imagery. Soil characteristics, including pH, organic matter content (OM), cation exchange capacity (CEC), soil texture, and soil type, were obtained from SoilGrids 2.0 for the 0–30 cm layer [19].

To assess the feasibility of cultivation, we compiled ten binary exclusion layers. Built-up land, water bodies, and wetlands were derived from ESA WorldCover 2021; roads and railways from national topographic data; and five categories of protected land (scientific research forest, landscape-protection areas, habitat- and species-conservation areas, nature reserves, and national parks) from the national special-use forest inventory, cross-checked against the World Database on Protected Areas. Each layer was rasterized onto the 30-m grid and applied within the mapped extent. No additional distance buffers were imposed, so the exclusion areas reported here are conservative with respect to linear infrastructure, which accounts for only 20,320 ha (0.22%) of the study area. The source, pixel count, and area of every layer are listed in Supplementary Table S13c. Exclusion of the special-use forest system follows the structure of the Law on Forestry No. 16/2017/QH14, which provides explicitly for combined agricultural and forestry production in protection forests (Article 57) and in production forests, but contains no equivalent provision for special-use forests, where permitted uses are limited to regulated harvesting, scientific research, teaching and ecotourism (Article 53). We treat this as a conservative bound rather than an absolute legal barrier: Article 54 permits households already holding residential or production land interspersed within a special-use forest but lying outside its approved plan to continue using that land, so limited cultivation may, in practice, be admissible at the margins of these areas.

Data preprocessing and harmonization

All spatial datasets were projected to a common coordinate system and resampled to the 30-m reference grid. Continuous variables were resampled using bilinear interpolation, whereas categorical variables were resampled using nearest-neighbor assignment. Resampling the approximately 1-km climatic layers and the 250-m soil layers onto the 30-m computational grid harmonizes the geometry of the input stack but does not create new spatial information at 30 m; boundary positions and area estimates therefore carry the uncertainty of the coarsest contributing layer, and areas are therefore reported as rounded estimates and should be interpreted at the effective resolution of the coarsest input layer. The environmental stack is also multi-temporal: the climate normals refer to 1981–2010, the SRTM elevation model to the 2000 acquisition, NDVI to a 2020–2023 median composite, and the soil and land-cover layers to 2021 (Supplementary Table S2). The baseline is therefore a multi-temporal composite rather than a strict 1981–2010 reconstruction; topographic and soil layers were held time-invariant, an assumption examined in the Limitations.

Several datasets require conversion from native storage units to physically meaningful values. CHELSA precipitation data were converted using the published scale factor, soil pH values were rescaled to conventional pH units, soil organic matter (OM) was estimated from soil organic carbon (SOC) using the Van Bemmelen factor, and SoilGrids cation exchange capacity (CEC) values were converted to $\mathrm{cmol_c\ kg^{-1}}$:

$$\mathrm{P(mm)} = \mathrm{raw} \times 0.1 \tag{1}$$

$$\mathrm{pH} = \mathrm{raw}/10, \mathrm{OM}(\%) = \frac{\mathrm{SOC\ (dg/kg)}}{100} \times 1.724 \tag{2}$$

$$\mathrm{CEC\ (cmol_c\ kg^{-1})} = \mathrm{raw}/100 \tag{3}$$

where Eqs. (1) and (2) apply the CHELSA scale and offset factors, and Eq. (3) applies the SoilGrids 2.0-unit conversion. Slope and aspect were derived from the DEM.

We generated topographic derivatives from the digital elevation model. We derived slope and aspect using standard terrain-analysis procedures. The topographic wetness index (TWI), representing the tendency of water accumulation, was calculated as:

$$\mathrm{TWI} = \ln\left(\frac{A_s}{\tan\beta}\right) \quad (4)$$

where β is the local slope in radians and A_s is the specific upslope contributing area. ESA WorldCover cells were resampled to 30 m resolution, and 10 binary spatial-constraint masks were generated for the exclusion analysis.

Ecological suitability classification

Each pre-processed criterion raster was reclassified into five suitability classes following the FAO land evaluation framework [20]: S1 = highly suitable (score 5), S2 = moderately suitable (4), S3 = marginally suitable (3), N1 = currently not suitable (2), and N2 = permanently not suitable (1). The classification thresholds for each criterion were established from published ecological characteristics of *Panax notoginseng* and regional suitability studies [5,21–23]. Supplementary Table S1 provides the full threshold table and the ecological rationale for each class boundary.

Literature-informed Fuzzy-AHP weighting

We quantified criterion importance using the Fuzzy Analytic Hierarchy Process (Fuzzy-AHP), which extends the conventional Analytic Hierarchy Process by incorporating uncertainty in pairwise comparisons through triangular fuzzy numbers (TFNs). We selected this method because the ecological importance scores underpinning the comparison matrix are uncertain, and triangular fuzzy numbers propagate that uncertainty through the weighting step.

This study did not include expert elicitation, so criteria such as panel composition or the number of participating experts does not apply. Instead, we assigned each of the fifteen criteria an importance score on a 1–9 scale, derived from the weights and importance statistics reported in previous suitability and distribution studies of P. notoginseng, with the specific basis for each criterion documented in Supplementary Table S14. The pairwise comparison matrix was generated from the ratios of these scores, rounded to the nearest integer on the Saaty 1–9 scale, with reciprocal values below the diagonal; a small number of near-boundary pairs, whose score ratios fell between 1.4 and 1.5, were assigned a value of 2 rather than 1 in order to preserve the ordering implied by the source studies. The mapping is therefore reproducible from the score table: 103 of the 110 off-diagonal entries follow directly from the rounded score ratios, and the seven near-boundary pairs are named in the caption of Supplementary Table S14. We then converted the matrix into TFNs using the Buckley fuzzy scale. Fuzzy weights were calculated using the geometric mean approach and then transformed into crisp values using the Best Non-Fuzzy Performance (BNP) method.

For each criterion i, the triangular fuzzy weight produced by the geometric-mean procedure has a lower, a modal, and an upper bound. These three bounds are converted into a single crisp value by the Best Non-Fuzzy Performance (BNP) method:

$$\mathrm{BNP}_i = w_i^l + \frac{[(w_i^u - w_i^l) + (w_i^m - w_i^l)]}{3} \quad (5)$$

where the superscripts *l*, *m*, and *u* denote the lower, modal, and upper bounds of the fuzzy weight of criterion *i*. The crisp values are then normalized to obtain the final criterion weights, $W_i = \mathrm{BNP}_i / \Sigma_j \mathrm{BNP}_j$ (j = 1, …, 15), which satisfy $\Sigma_i W_i = 1$.

We evaluated the consistency of the comparison matrix using the consistency ratio (CR), with values below 0.10 considered acceptable. For the defuzzified comparison matrix on which the weights are computed, CR = 0.0402 (λ_{max} = 15.895; CI = 0.0639; RI = 1.59), and the crisp Saaty matrix itself has CR = 0.0081. Supplementary Tables S3, S3b, and S4 present the full crisp comparison matrix, its triangular fuzzy number form, and the resulting global weights.

Ecological suitability modeling

We quantified environmental suitability using a weighted fuzzy-overlay model that integrates each environmental criterion's relative importance with its degree of suitability. The suitability index at the location p was computed as:

$$SI(p) = \left[\sum_{i=1}^{15} W_i \, \mu_i(p)\right] \times C_{MAT}(p) \times C_{DEM}(p) \times C_{SLP}(p) \qquad (6)$$

where W_i represents the normalized criterion weight, $\mu_i(p)$ is the fuzzy membership value, and C_k denotes non-compensatory ecological constraints.

We implemented three ecological veto criteria (mean annual temperature, elevation, and slope) as Boolean filters. Locations classified as permanently unsuitable (N2) for any of these variables were excluded regardless of performance in other criteria. This approach prevents unrealistic compensation among environmental variables and preserves critical ecological thresholds governing species survival.

The continuous index was classified at the membership-function breakpoints:

$$\mathrm{Class}(p) = \begin{cases} \mathrm{S1} & 0.75 < \mathrm{SI} \leq 1.00 \\ \mathrm{S2} & 0.50 < \mathrm{SI} \leq 0.75 \\ \mathrm{S3} & 0.25 < \mathrm{SI} \leq 0.50 \\ \mathrm{N1/N2} & 0 \leq \mathrm{SI} \leq 0.25 \\ \mathrm{N2} & \mathrm{SI} = 0 \end{cases} \qquad (7)$$

Future Climate Suitability Projections

The five climatic criteria were re-projected for 2041–2070 under two Shared Socioeconomic Pathway–Representative Concentration Pathway scenarios, SSP3-7.0 and SSP5-8.5 [6,15,16,24,25], using CHELSA-CMIP6 downscaled data from five general circulation models (GCMs): GFDL-ESM4, IPSL-CM6A-LR, MPI-ESM1-2-HR, MRI-ESM2-0, and UKESM1-0-LL [26]. Eq. (6) was computed for each GCM, and the per-model suitability surfaces were combined into an ensemble mean for each scenario. We held the topographic and soil layers time-invariant. All five GCMs and both scenarios were weighed equally. In the absence of an objective, regionally validated measure of relative model skill for this study area, equal weighting avoids imposing a priori preference among projections and is consistent with standard ensemble practice. Model-related and scenario-related uncertainty are reported separately in the Results: dispersion among the five GCMs is summarised by the per-cell coefficient of variation and standard deviation, and the number of cells reaching each per-class consensus count is tabulated in Supplementary Table S12, whereas the contrast expresses scenario-related uncertainty in suitable area between SSP3-7.0 and SSP5-8.5 (Supplementary Table S5).

Climate-stability and consensus analysis

Across the ten future suitability maps (5 GCMs × 2 SSPs), the per-class consensus frequency at each cell was defined as:

$$\mathrm{freq}_c(x) = \sum_{s=1}^{10} 1\,[\mathrm{class}_s(x) = c], \qquad c \in \{S1, S2, S3\} \tag{8}$$

where $\mathrm{freq}_{S1} + \mathrm{freq}_{S2} + \mathrm{freq}_{S3} + \mathrm{freq}_N = 10$ over all valid cells. Climate-stable S1 core zones were delineated at nested consensus thresholds $\tau \in \{1, \ldots, 10\}$:

$$\mathrm{Core}(\tau) = \left\{ x : \mathrm{class}_{base}(x) = S1 \ \wedge \ \mathrm{freq}_{S1}(x) \geq \tau \right\} \tag{9}$$

For interpretation, cells satisfying $\tau \geq 8/10$ were designated climate-stable cultivation refugia. Cells satisfying lower consensus thresholds were retained as candidate zones with lower confidence. This terminology is operational and refers to model-based decision-support zones rather than empirically verified demographic refugia. The migration zone, defined as areas changing from S2 under baseline to S1 under future consensus, was mapped separately. The area of each class (km²) by scenario and the consensus-frequency distribution were tabulated.

Land-use-feasible cultivation zones

The long-term available cultivation zone at the consensus threshold τ is the intersection of the stable S1 core with the complement of the spatial exclusion mask:

$$\mathrm{Avail}(\tau) = \mathrm{Core}(\tau) \ \cap \ \neg\, \mathrm{Exclusion} \tag{10}$$

An area budget (core area, area removed by physical constraints, area removed by conservation constraints, and net available area) was computed for each τ.

Model evaluation and predictor-sensitivity analysis

Because the suitability model is deductive (its thresholds and weights are derived from published ecological knowledge rather than fitted to occurrence data), the 27 occurrence records were used exclusively for independent external evaluation and played no part in calibration. The records were compiled from published Vietnamese studies of P. notoginseng, with each record attributed to its source publication in Supplementary Table S15; no records were obtained from GBIF, and no primary field survey was undertaken for this study. Seven records carry exact GPS coordinates as reported in the source study and are flagged as high positional quality; the remaining twenty are commune-, district-, or province-level centroids inferred from occurrence descriptions and are flagged as medium or low positional quality. Records were screened for duplicate coordinates, and the elevation stated in each source was compared with the elevation of the digital elevation model at the recorded location as an objective check of positional accuracy. Spatial thinning was not applied because the records are dispersed across four provinces and show no clustering at the resolution of the analysis. Population status (wild, cultivated, or experimental) is not consistently reported in source literature and is recorded as unspecified. Discriminatory ability was quantified with the area under the receiver operating characteristic curve (AUC) and the continuous Boyce index, using a presence–background design with 10,000 background points drawn by latitude-stratified random sampling (ten strata; random seed 20240601); confidence limits for the AUC were obtained from 2,000 bootstrap resamples. Both metrics are appropriate for presence-only data. We did not compute the

true skill statistics or Cohen's kappa, as they require verified absence records and a binary threshold, neither of which is available for this dataset.

Potential multicollinearity among predictors was assessed using Pearson correlation coefficients and variance inflation factors (VIFs) at 10,000 latitude-stratified sample points. VIFs were computed in two spaces: on the raw predictor values and on the reclassified and fuzzified layers that actually enter the weighted overlay. Because the model operates on the latter, the operational values are the diagnostically relevant ones (Supplementary Table S7). To test whether the weighting structure itself predetermines the outcome, the complete overlay was additionally recomputed over the entire study area using two reduced predictor sets: M1, excluding elevation; and M2, excluding elevation and the maximum and minimum temperature layers, so that mean annual temperature is the sole thermal predictor. In both cases, the remaining weights were renormalized to sum to unity, and the non-compensatory vetoes were left unchanged, which isolates the effect of redundant weighting from that of the ecological constraints. The reduced surfaces were compared with the full model using class agreement, Cohen's kappa, Spearman rank correlation for the continuous index, and Jaccard overlap for the S1 class (Supplementary Table S16).

Weight-sensitivity analysis

The robustness of the suitability model was evaluated using a one-at-a-time sensitivity analysis. Criterion weights were systematically perturbed while maintaining the total weight equal to unity. The resulting changes in ranking were used to assess the stability of the weighting structure and identify parameters with the greatest influence on model outcomes.

Reproducibility

All analyses were performed in ArcGIS Pro 3.7, Google Earth Engine, and R. Complete source code, processed datasets, and model outputs have been archived in a publicly accessible repository to ensure transparency and reproducibility. The study reports no new algorithm or software package; the analysis is assembled from documented operations in these established tools, and the R code that reproduces the results, organized by analysis stage, is deposited in the record given under Code availability.

RESULTS

Climatic controls dominate ecological suitability

The Fuzzy-AHP analysis produced a consistent weighting structure (CR = 0.0402), indicating acceptable internal consistency of the decision matrix. Climatic variables dominated the ranking, with mean annual temperature receiving the highest weight (W = 0.1230), followed by minimum temperature of the coldest month and elevation (W = 0.1177 each), annual precipitation (W = 0.1051), and maximum temperature of the warmest month (W = 0.0672). Together, these variables accounted for more than half of the total weight assigned to the suitability model. In contrast, soil and terrain-related factors generally received lower weights.

The dominance of thermal variables highlights the strong climatic sensitivity of *Panax notoginseng* and suggests that future temperature changes may represent the primary driver of habitat redistribution (Supplementary Table S4). Weight sensitivity analysis showed that the composition of the leading group remained stable under substantial perturbations, indicating that the climate-dominated hierarchy is robust, although the internal order of the leading criteria is not itself claimed to be robust (Supplementary Table S6). Because the four temperature- and elevation-related predictors are strongly correlated in their raw form, we verified that this ranking is not an artefact of redundant weighting: in the operational space on

which the overlay is computed, all variance inflation factors fall below the conventional threshold of 10 (maximum 9.01; Supplementary Table S7), and recomputing the overlay over the whole study area with elevation removed (M1), and with elevation, maximum and minimum temperature removed (M2), left the class ranking unchanged (class agreement 96.4% and 93.1%). The extent of the highly suitable class is less stable (Jaccard overlap 60.6% and 23.1%), and the climate-stable core is less stable again, retaining 34.8% and 10.1% of the full-model area at $\tau \geq 8/10$ (Supplementary Table S16).

Current suitability is spatially restricted

Under baseline climatic conditions (1981–2010), highly suitable land (S1) occupied approximately 7,250 km², representing 7.9% of the valid study area. Moderately suitable land (S2) accounted for approximately 31,700 km² (34.5%), whereas marginally suitable land (S3) covered approximately 115 km² (0.1%). More than half of the study area (57.5%) was classified as permanently unsuitable (N2).

The most suitable areas were concentrated primarily in elevated mountainous regions with favorable thermal and moisture conditions. The limited extent of S1 land indicates that suitable cultivation environments for *P. notoginseng* are already geographically constrained under present climatic conditions (Figure 3).

Comparison with the unconstrained weighted-overlay model revealed the strong influence of ecological veto criteria. Removal of the Boolean ecological constraints expanded the moderately suitable class about 2.5-fold (to approximately 78,000 km²) and the marginally suitable class about 57-fold (to approximately 6,600 km²), whereas the highly suitable area changed only marginally, from approximately 7,250 to 7,470 km² (Supplementary Table S5; Supplementary Figure S3). The vetoes therefore act almost entirely on cells that the compensatory model had placed in the moderately and marginally suitable classes. This is a property of the classification rule rather than independent evidence about the realized niche of the species.

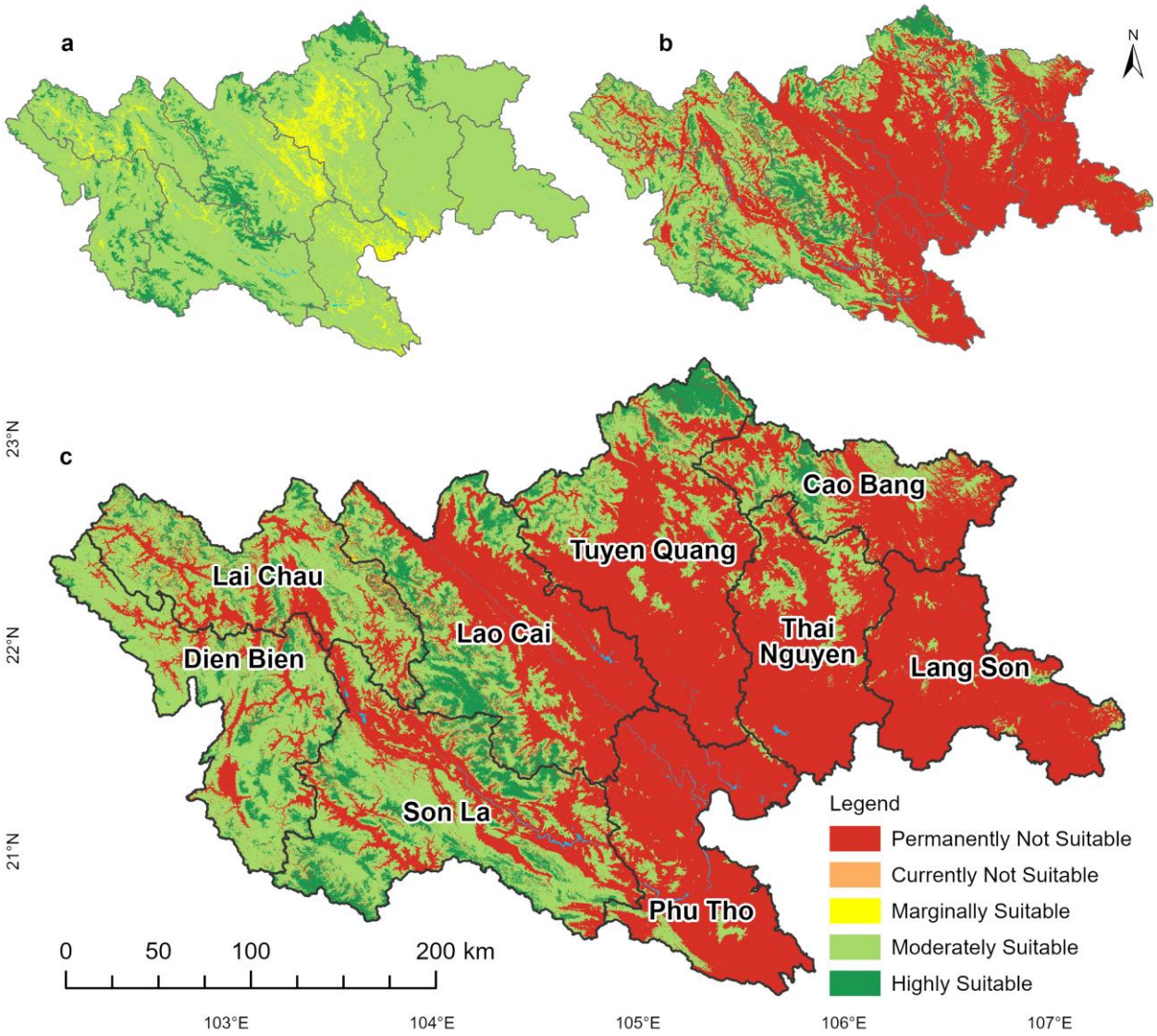


Figure 3. Current ecological suitability (1981–2010) of *Panax notoginseng* in northern mountainous Vietnam. (a) Compensatory weighted-overlay model without ecological constraints; (b–c) non-compensatory suitability model incorporating ecological veto criteria for temperature, elevation, and slope. Suitability classes range from highly suitable (S1) to permanently unsuitable (N2). Maps were created by the authors in ArcGIS Pro 3.7 (Esri; https://www.esri.com/en-us/arcgis/products/arcgis-pro/).

Climate warming substantially reduces highly suitable cultivation land

Future climate projections consistently indicated a pronounced reduction in highly suitable habitat across all climate models and emission scenarios. Under SSP3-7.0, the ensemble mean projected a decline in the S1 area from approximately 7,250 km² to 2,330 km², corresponding to a 68% reduction relative to the baseline. Under SSP5-8.5, the highly suitable area decreased further to approximately 1,580 km², representing an approximate 78% reduction. These reductions raise questions about the long-term viability of *Panax notoginseng* cultivation and emphasize the need for adaptive planning strategies.

At the same time, marginally suitable land expanded substantially under both scenarios. The expansion of S3 and contraction of S1 indicate a progressive degradation of cultivation conditions rather than a simple redistribution of suitable habitat. Although inter-model variability remained considerable, all five CMIP6

models projected the same overall trend of habitat loss, demonstrating that the contraction signal is consistent across models and robust to climate-model uncertainty (Figure 4).

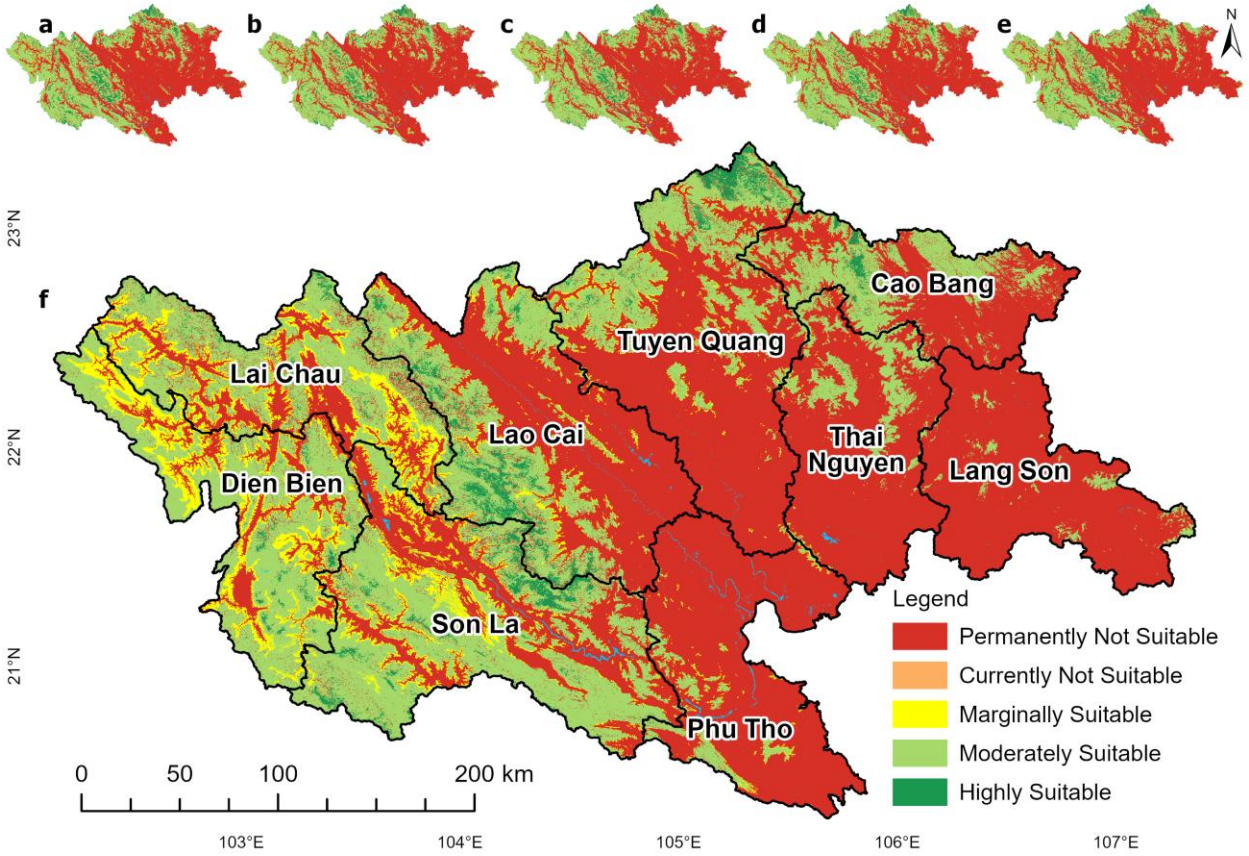


Figure 4. Future ecological suitability of *Panax notoginseng* under SSP3-7.0 (2041–2070). Panels (a–e) show projections from five CMIP6 climate models, and panel (f) shows the ensemble mean. Suitability classes range from highly suitable (S1) to permanently unsuitable (N2). Maps were created by the authors in ArcGIS Pro 3.7 (Esri; https://www.esri.com/en-us/arcgis/products/arcgis-pro/).

The stronger decline observed under SSP5-8.5 further demonstrates the species' clear sensitivity to warming intensity, indicating that future emissions trajectories may strongly influence the extent of remaining cultivation opportunities (Figure 5).

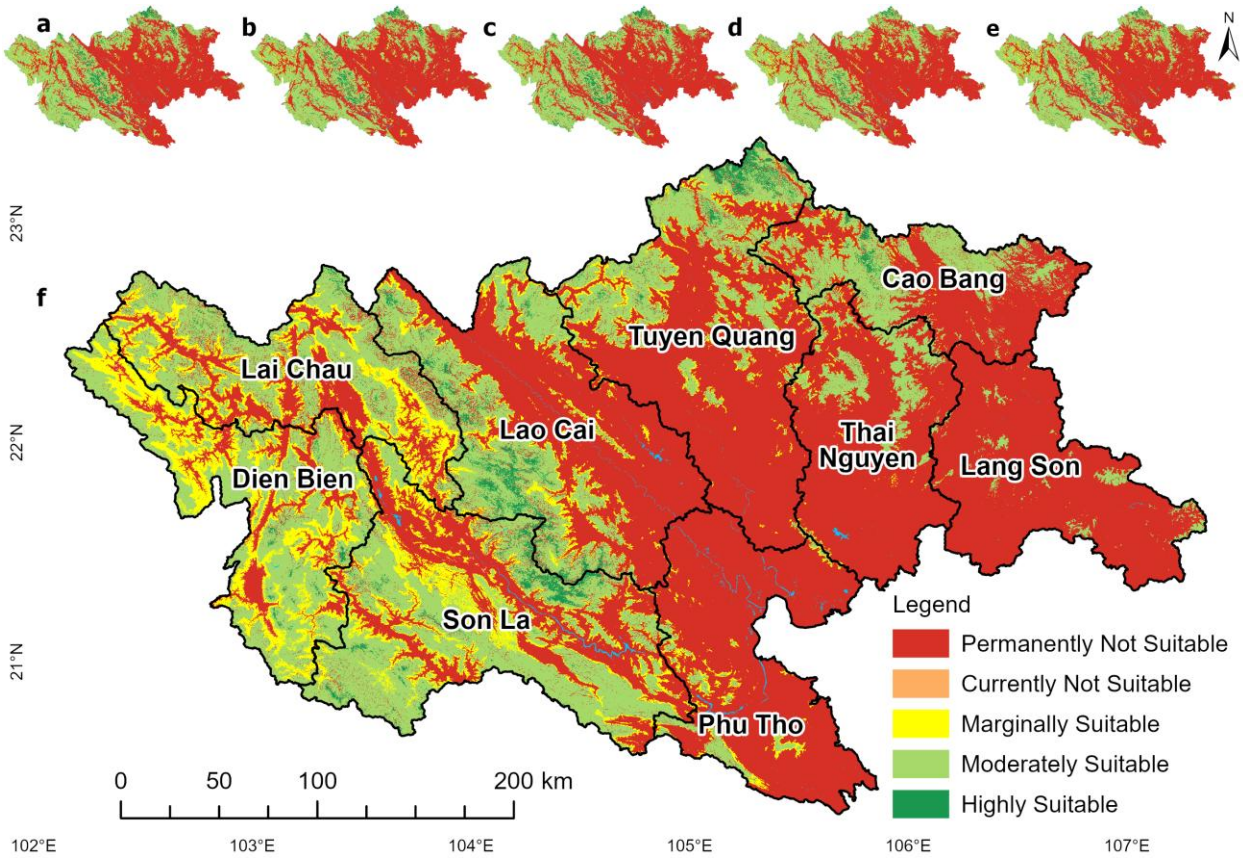


Figure 5. Future ecological suitability of *Panax notoginseng* under SSP5-8.5 (2041–2070). Panels (a–e) show projections from five CMIP6 climate models, and panel (f) shows the ensemble mean. Suitability classes range from highly suitable (S1) to permanently unsuitable (N2). Maps were created by the authors in ArcGIS Pro 3.7 (Esri; https://www.esri.com/en-us/arcgis/products/arcgis-pro/).

Inter-model uncertainty in future suitability projections

Future suitability projections showed substantial spatial variability across climate models, underscoring the importance of explicitly quantifying uncertainty. Figure 6 presents the ensemble mean suitability, coefficient of variation (CV), standard deviation (SD), and model consensus across all projections.

The ensemble-mean suitability map (Figure 6a) indicates that climatically favorable environments remain concentrated in high-elevation mountainous regions. However, the uncertainty maps reveal considerable spatial heterogeneity in model agreement, highlighting areas where habitat projections are less reliable and warranting caution in conservation planning. Elevated uncertainty (high CV and SD values) is primarily observed along suitability transition zones and mountainous margins. In contrast, the central highland regions generally exhibit lower variability among projections (Figures 6b and 6c).

The consensus analysis further demonstrates that model agreement is not uniformly distributed across the landscape (Figure 6d). Areas exhibiting high agreement (90–100%) represent locations where future suitability predictions remain relatively robust across climate models and emission scenarios. In contrast, regions with low agreement are more sensitive to climate-model assumptions and should therefore be interpreted with caution.

These results demonstrate that future suitability should not be evaluated solely based on ensemble means. Explicit representation of model uncertainty provides additional information for identifying robust cultivation opportunities and supports more reliable adaptation planning under climate change.

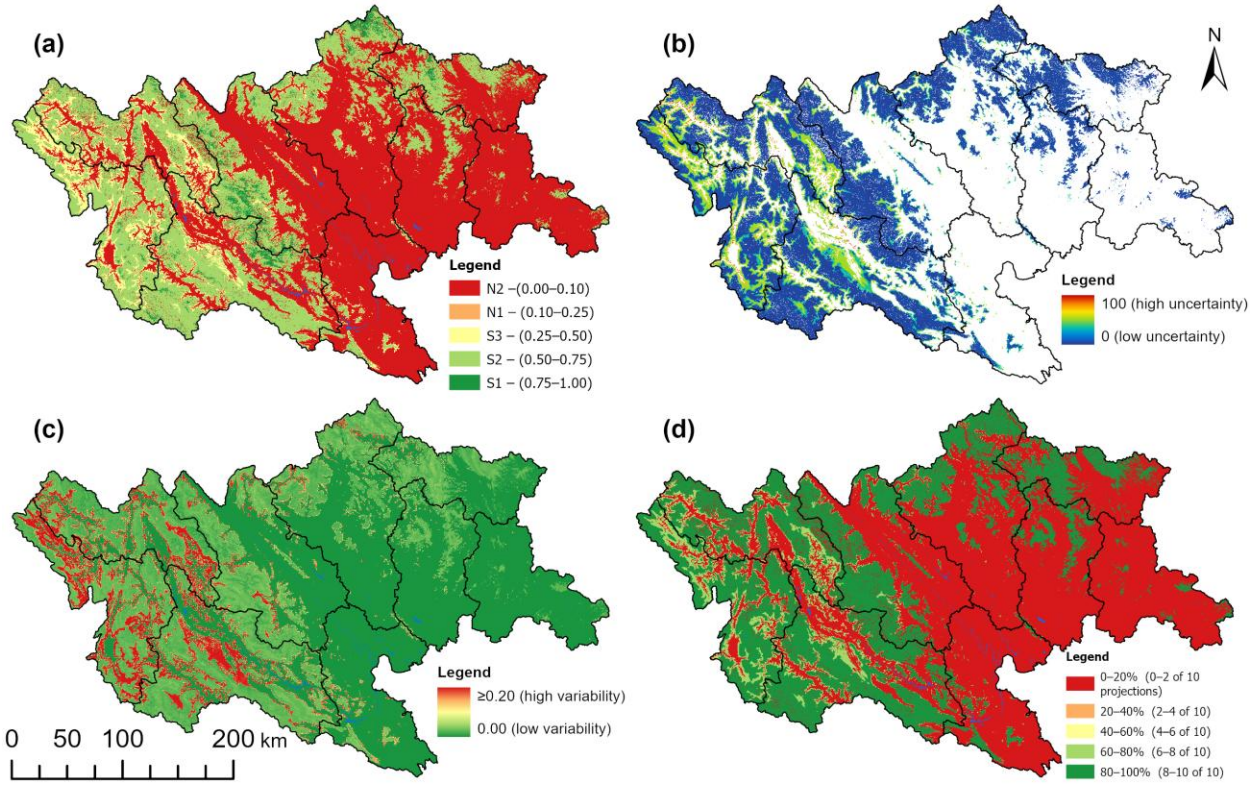


Figure 6. Inter-model uncertainty in future ecological suitability of *Panax notoginseng* (2041–2070). Maps show (a) ensemble mean suitability, (b) coefficient of variation (CV), (c) standard deviation (SD), and (d) model–scenario consensus across ten future projections (five CMIP6 models × two emission scenarios). High CV and SD values indicate greater uncertainty, whereas high consensus values indicate more robust suitability predictions. Maps were created by the authors in ArcGIS Pro 3.7 (Esri; https://www.esri.com/en-us/arcgis/products/arcgis-pro/).

Climate-stable refugia occupy only a small fraction of future habitat

While ensemble projections identified extensive areas that remained suitable under at least one future scenario, consensus analysis revealed that only a relatively small proportion of these areas remained consistently suitable across models and scenarios.

The highly suitable climate-stable core declined from approximately 3,830 km² at the lowest consensus threshold (τ = 1/10) to approximately 139 km² under full model–scenario agreement (τ = 10/10). We designate cells meeting $\tau \geq 8/10$as climate-stable cultivation refugia and describe cells identified only at lower thresholds as candidate, lower-confidence zones. These areas are model-based planning priorities rather than empirically verified demographic refugia. This represents a reduction of more than 96% between the least and most conservative definitions of climate stability. This decline underscores the importance of identifying potential migration zones to sustain cultivation opportunities amid changing climates.

The analysis also identified potential migration zones, defined as areas currently classified as moderately suitable that are projected to become highly suitable under future conditions. These zones reached approximately 722 km² under weak consensus but decreased substantially as agreement requirements increased.

These findings demonstrate that future suitability alone may substantially overestimate long-term cultivation opportunities. Areas consistently identified as suitable by multiple climate models are considerably smaller than those indicated by individual projections, highlighting the importance of explicitly accounting for climate uncertainty in agricultural planning (Figure 7).

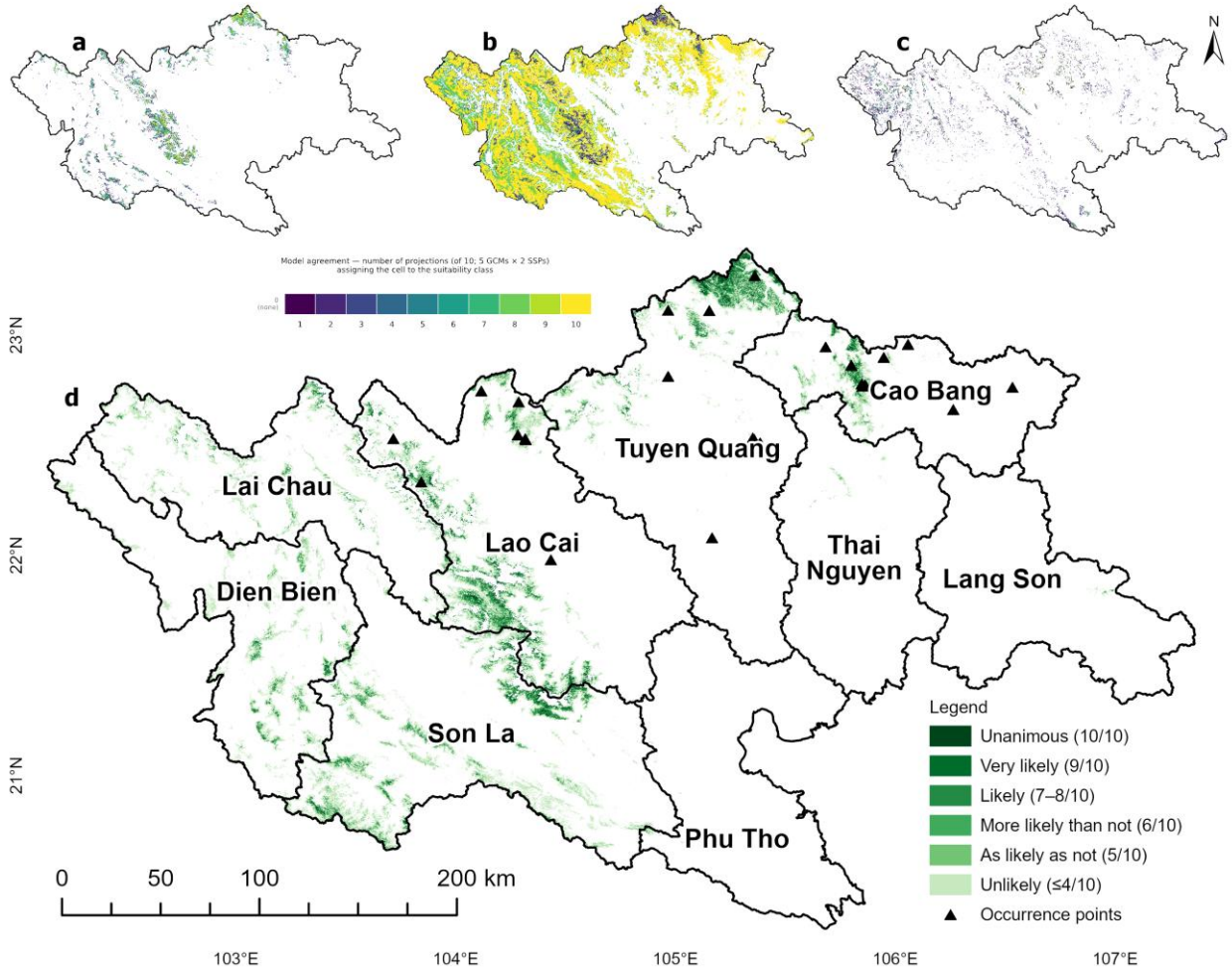


Figure 7. Climate-stable refugia of *Panax notoginseng* identified through multi-model consensus. Panels (a–c) show consensus frequencies for highly suitable (S1), moderately suitable (S2), and marginally suitable (S3) classes across ten future projections. Panel (d) shows climate-stable refugia, classified by the level of agreement among climate models and emission scenarios. Maps were created by the authors in ArcGIS Pro 3.7 (Esri; https://www.esri.com/en-us/arcgis/products/arcgis-pro/).

Land-use constraints further reduce feasible cultivation opportunities

Intersecting climate-stable cores with the spatial exclusion masks yielded the long-term available cultivation zones. The available area decreased from approximately 3,360 km² at $\tau = 1/10$ to approximately 127 km² under full consensus. A notable finding was that most excluded land was due to conservation constraints rather than physical barriers. Under near-full consensus ($\tau \geq 9/10$), conservation-designated areas accounted for more than 96% of the excluded area, whereas built-up land, roads, and other physical constraints contributed only a minor fraction (Figure 8).

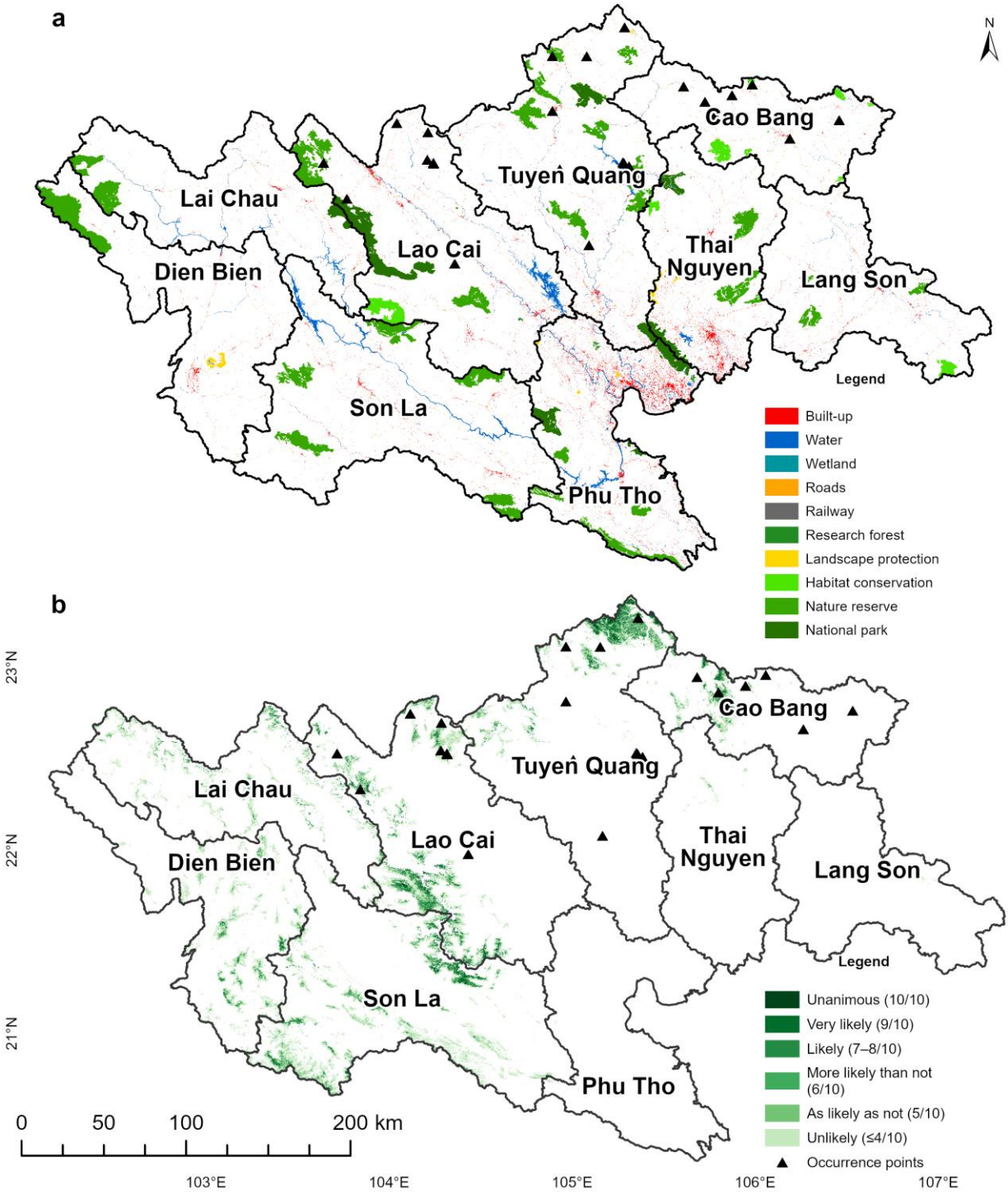


Figure 8. Climate-stable and land-use-feasible cultivation zones for *Panax notoginseng*. (a) Spatial exclusion layers used to identify unavailable land, including physical and conservation constraints. (b) Final cultivation zones obtained by intersecting climate-stable refugia with land-use availability masks, classified according to model–scenario agreement. Maps were created by the authors in ArcGIS Pro 3.7 (Esri; https://www.esri.com/en-us/arcgis/products/arcgis-pro/).

This result reveals a potential tension between medicinal plant cultivation and biodiversity conservation. Many of the most climatically stable locations coincide with protected landscapes, suggesting that future expansion of cultivation may require a careful balance between conservation objectives and sustainable medicinal-plant development.

Validation and model robustness

Multicollinearity analysis identified strong correlations among temperature- and elevation-related predictors in their raw form ($|r| \geq 0.93$; Supplementary Table S8 and Supplementary Figures S9 and S10). In the operational space on which the overlay is computed, all variance inflation factors fell below the exclusion threshold, and the reduced-model comparison showed that the overall class pattern remained broadly similar, although the S1 boundary and high-consensus core were sensitive to predictor specification (Supplementary Table S16).

Evaluation against the 27 published occurrence records yielded an area under the ROC curve (AUC) of 0.683 (95% confidence interval 0.581–0.779; 2,000 bootstrap resamples) and a continuous Boyce index of 0.925 (Supplementary Table S9). The AUC indicates modest discriminative ability, whereas the high Boyce index indicates that the predicted-to-expected ratio increases monotonically with the suitability score (Supplementary Figure S8); this is not a statement about the modal class of the records (Supplementary Table S10a). Eight of the 27 records fall in cells classified as permanently unsuitable, seven are vetoed by elevation, and one by slope, and all eight have centroid or inferred coordinates; none of the seven records with exact published GPS coordinates are vetoed (Supplementary Table S15). Those seven agree with the digital elevation model to within 4–21 m of their published elevations, whereas the model gives 97–584 m at the elevation-vetoed coordinates, far below the range documented for the species, but precisely where district and provincial centroids fall, since administrative centres lie in valleys rather than on cultivated slopes. These vetoes therefore track positional error rather than threshold failure, although with only seven exact records, the association is not statistically conclusive (one-sided Fisher's exact test, $p = 0.07$). Because both metrics were computed across all 27 records, the reported values are lower bounds. On the seven exact records alone, the AUC is 0.890 and the Boyce index 0.903 (Supplementary Table S18).

These results indicate that the surface ranks known occurrences sensibly at broad scale rather than predicting suitability at site level.

DISCUSSION

This study demonstrates that future cultivation planning for climate-sensitive medicinal plants cannot rely solely on present-day suitability assessments. By integrating ecological suitability, climate projections, model–scenario consensus, and land-use feasibility, we show that the area potentially available for sustainable cultivation of *Panax notoginseng* is substantially smaller than conventional suitability mapping suggests. Although large areas remain suitable in individual future projections, only a relatively small

fraction remains climate-stable and practically available for cultivation when uncertainty and land-use constraints are explicitly considered. These findings highlight the importance of moving beyond static suitability assessments toward climate-resilient cultivation planning frameworks.

Climatic controls govern the distribution of *Panax notoginseng*

The dominance of temperature-related variables in the Fuzzy-AHP weighting structure confirms the strong climatic dependence of *P. notoginseng*. Mean annual temperature, minimum temperature of the coldest month, elevation, and annual precipitation collectively accounted for the largest proportion of the total suitability weight, indicating that thermal and moisture conditions are the primary environmental controls governing species distribution. This result is consistent with the ecological characteristics of *P. notoginseng*, which is adapted to cool, humid mountain environments and exhibits limited tolerance to elevated temperatures [5].

The strong influence of thermal variables is also biologically plausible. Temperature regulates physiological processes, including photosynthesis, respiration, water-use efficiency, root development, and secondary metabolite production. Previous studies have demonstrated that both yield and ginsenoside accumulation are sensitive to thermal and moisture conditions [27–29]. Consequently, even modest climatic shifts may alter habitat suitability, particularly near the margins of the species' ecological niche. The stability of the ranking structure under sensitivity analysis further suggests that the dominance of climatic variables is not an artifact of subjective weighting but reflects fundamental ecological control. Mechanistically, warming acts on this shade-adapted understorey herb by imposing thermal stress on photosynthesis, root development, and saponin accumulation, rather than through light availability alone, which is why the thermal criteria carry the greatest weight.

Current cultivation opportunities are already limited

Under present climatic conditions, highly suitable land represents less than 8% of the study area, indicating that optimal cultivation environments are already geographically restricted. The strong influence of ecological veto criteria further demonstrates that many locations fail to satisfy critical environmental requirements despite exhibiting favorable conditions for some individual variables.

This finding reinforces the importance of considering ecological thresholds rather than relying solely on compensatory suitability models. In mountain environments, climatic, topographic, and soil constraints often interact nonlinearly, and favorable conditions in one variable cannot necessarily offset severe limitations in another. The relatively small extent of highly suitable land, therefore, reflects the ecological specialization of *P. notoginseng* and highlights its inherent vulnerability to environmental change.

Climate warming is projected to substantially reduce suitable habitat

All climate projections indicated a marked contraction in highly suitable habitat by mid-century, with the largest reductions under the high-emission SSP5-8.5 scenario. The consistent decline across all climate models suggests that habitat contraction is a robust consequence of warming rather than an artifact of individual model behavior.

The projected losses are consistent with broader observations of climate-driven range shifts in mountain ecosystems. As temperatures increase, suitable thermal conditions tend to migrate upslope, while lower-

elevation habitats become increasingly unsuitable. However, mountain species often face a finite elevational limit, creating a phenomenon sometimes referred to as the "escalator to extinction," whereby suitable habitat progressively shrinks as species are forced toward mountain summits [7,30]. For species such as *P. notoginseng*, which already occupy relatively narrow environmental niches, this process may substantially reduce future cultivation opportunities and increase production vulnerability.

Similar contractions have been reported for *Panax pseudoginseng* in the Himalayan region, where future climate scenarios projected substantial reductions in suitable habitat and increasing fragmentation of cultivation areas [9]. Comparable trends have also been observed for other mountain medicinal plants, for which warming-induced shifts in temperature and precipitation regimes are expected to reduce habitat suitability and threaten long-term sustainability [8]. However, unlike previous studies that primarily focused on mapping future suitability, the present framework explicitly distinguishes climate-stable refugia and land-use-feasible cultivation zones by integrating multi-model climate consensus and spatial exclusion constraints. This distinction provides a more robust basis for long-term cultivation planning under uncertainty and reduces the risk of overestimating future cultivation opportunities.

Importantly, the stronger contraction observed under SSP5-8.5 suggests that future emissions trajectories will play a critical role in determining the extent of remaining suitable habitat. This finding emphasizes the broader connection between climate mitigation efforts and the long-term sustainability of medicinal plant resources [6].

Importance of uncertainty-aware cultivation planning

A major challenge in climate adaptation planning is the substantial uncertainty associated with future climate projections. Many previous suitability studies rely primarily on ensemble averages, which may conceal important disagreement among climate models [31]. The uncertainty analysis presented here demonstrates that suitability projections are spatially heterogeneous not only in their predicted suitability but also in their associated confidence.

Areas exhibiting low variability and high model agreement can be interpreted as higher-confidence cultivation candidates conditional on the selected models, scenarios, thresholds, and predictor specification, whereas areas characterized by high variability warrant more cautious interpretation. Consequently, uncertainty itself becomes a useful decision variable rather than merely a limitation of the modeling process. The spatial structure of model disagreement is itself informative: dispersion is highest along the margins of the massifs and across class transitions, where a small thermal offset moves a cell across a threshold, and lowest in the high-elevation interiors that form the stable core.

By explicitly quantifying the coefficient of variation, standard deviation, and model consensus, the present framework transforms climate uncertainty into actionable spatial information. This approach provides a more transparent basis for long-term agricultural planning and reduces the risk of maladaptation arising from overreliance on individual climate projections.

Climate-stable refugia support robust adaptation planning

A key contribution of this study is the identification of climate-stable refugia through model–scenario consensus analysis. Traditional suitability assessments typically emphasize average projections, which can obscure substantial uncertainty among climate models. In contrast, the consensus-based approach explicitly

identifies areas that remain suitable across multiple models and scenarios, thereby converting uncertainty into actionable spatial information [31].

The results reveal that climate-stable refugia occupy only a small fraction of the area classified as suitable under individual projections. This finding suggests that future cultivation planning based solely on projected suitability may substantially overestimate the availability of reliable cultivation environments. Areas consistently identified as suitable across diverse climate futures are likely to provide more robust long-term investment opportunities and may therefore represent priority locations for cultivation expansion, germplasm conservation, and adaptation planning.

Beyond *P. notoginseng*, the concept of climate-stable cultivation refugia may have broad applicability to other climate-sensitive crops and medicinal plants. As climate uncertainty becomes increasingly important for agricultural planning, consensus-based refugia approaches could provide a valuable framework for identifying locations that remain resilient under multiple future conditions.

Land-use constraints reveal a cultivation–conservation trade-off

An important finding is that many climate-stable cultivation refugia overlap with protected and conservation-designated land. Consequently, the area that is both climatically suitable and potentially available for cultivation is smaller than ecological suitability alone would indicate. This overlap creates a potential trade-off between medicinal-plant development and biodiversity conservation, because protected mountain landscapes often coincide with the cool, humid conditions favorable for *P. notoginseng* cultivation.

Translating a suitability surface into a planning decision requires an explicit allocation rule. In this study, we used a binary exclusion mask to provide a transparent and precautionary first-pass screen for areas where cultivation is unlikely to be feasible or appropriate. This approach differs from more differentiated land-use zoning frameworks. For example, Esen et al. [32] developed a hybrid rule-based and machine-learning approach that converts social–ecological indicators into multiple operational zoning classes and treats disagreement between zoning approaches in transitional landscapes as a signal for targeted field investigation. Similarly, Adiguzel et al.[33] used explainable modeling and NSGA-II multi-objective optimization to examine conservation–development trade-offs and demonstrate the value of explicitly representing intermediate or controlled-use land-allocation options. The binary exclusion mask was also applied as a conservative planning screen informed by Vietnam's Law on Forestry No. 16/2017/QH14 [36], which establishes differentiated management and use regimes for forest categories. Special-use forest areas were treated conservatively in the exclusion analysis because activities within such areas are subject to statutory restrictions and approved management arrangements under the Forestry Law (Articles 53–54).

Our binary mask is not intended to replace such multi-objective zoning or site-level land-allocation analysis. Rather, it identifies where those more detailed assessments are most needed. Across consensus thresholds, land-use exclusions removed 8–12% of the climate-stable core, and 94–97% of the excluded area was conservation-designated rather than physically constrained. At $\tau \geq 9/10$, nature reserves and national parks accounted for 33.7 km² of the 37.3 km² excluded from the stable core (Supplementary Tables S13a–b). Thus, the conservation–cultivation trade-off is spatially limited in area but important for planning because it is concentrated in the most strictly protected categories.

These overlaps should be interpreted as priority locations for site-specific assessment rather than automatic approvals or prohibitions. Any future cultivation decision should verify forest category, approved management plans, land tenure, local regulations, and the potential for low-impact cultivation or conservation-compatible agroforestry. Vietnam's Forestry Law provides differentiated rules for forest categories and activities, including provisions for research and ecotourism in special-use/reserve forests and for regulated agroforestry in protection forests; the practical applicability of these provisions depends on local legal and management conditions.

Rather than treating protected-area overlap solely as a constraint, future planning could examine opportunities for germplasm conservation, community-based cultivation outside strictly protected cores, or carefully regulated agroforestry where legally permissible. Where future warming crosses ecological thresholds, climate-stable areas may offer higher-confidence locations for evaluating adaptation or relocation options. However, field validation of plant performance, ecological impacts, tenure, market access, and household-level feasibility are required before site-level implementation.

Uncertainty, limitations, and future directions

Several sources of uncertainty should be considered when interpreting these results. First, we evaluated the model against 27 occurrence records compiled from published literature rather than a dedicated field campaign. Seven have exact GPS coordinates; the remainder are administrative centroids whose positional error can shift a record across the study area's steep gradients. A systematic field survey at accurately known coordinates (recording presence, cultivation performance, microclimate, soil properties, and management practice) remains the most valuable next step, and the present analysis offers no substitute for it [34].

Second, we observed strong correlations among temperature- and elevation-related predictors in their raw form. They were retained because they represent distinct ecological mechanisms, because their variance inflation factors fall below the exclusion threshold in the operational space, and because the reduced-model comparison showed that the mapped pattern was insensitive to their removal [35]. The residual covariation means that the boundary between the highly and moderately suitable classes is less certain than the extent of suitable land as a whole, and that the absolute area of the climate-stable core is conditional on the full fifteen-criterion specification.

Third, future projections were based on five climate models, two emission pathways, and a single mid-century time horizon. Although this framework captures a substantial range of climate uncertainty, future studies could incorporate additional scenarios, longer-term projections, and dynamic land-use change. Similarly, soil and topographic conditions were assumed to remain constant over time, whereas future environmental changes may alter local site conditions. In addition, the effective information resolution is coarser than the 30-m computational grid: the climatic predictors are native to approximately 1 km, so class boundaries are smoother in reality than they appear and areas are reported rounded; aggregating the baseline surface to 240, 510 and 990 m changes the highly suitable class by at most 0.08 percentage points of the valid area (Supplementary Table S19). The baseline is also a multi-temporal composite, since the vegetation and land-cover layers describe present-day conditions rather than those of the climate-normal period.

Finally, ecological suitability does not necessarily guarantee successful cultivation. Factors such as accessibility, land tenure, infrastructure, economic viability, management practices, and market conditions were beyond the scope of this study but will influence practical implementation. Integrating socioeconomic

and ecological dimensions represents an important direction for future research. Taking together, these limitations mean the outputs are decision-support surfaces with quantified uncertainty rather than deterministic forecasts, and the reported areas are specification-dependent upper bounds on confidence rather than planning figures.

CONCLUSIONS

This study developed an uncertainty-aware geospatial framework for climate-resilient cultivation planning of *Panax notoginseng* in the mountainous regions of northern Vietnam. The framework integrates literature-informed GIS-based Fuzzy Analytic Hierarchy Process (Fuzzy-AHP) modelling, non-compensatory ecological constraints, CMIP6 climate projections, cross-projection consensus analysis, and land-use feasibility screening. It distinguishes between ecological suitability, climate stability, and land-use-feasible cultivation opportunities.

Land classified as highly suitable for cultivation covered approximately 7,250 km² under baseline conditions but declined to approximately 2,330 km² under SSP3-7.0 and 1,580 km² under SSP5-8.5 by 2041–2070. Areas retained as highly suitable across alternative future projections were much smaller: the baseline S1 stable core decreased from approximately 3,830 km² at the weakest consensus threshold to 139 km² under full model–scenario agreement. After land-use exclusions, potentially available cultivation land ranged from approximately 3,360 km² to 127 km² across consensus thresholds. Thus, increasingly stringent model–scenario agreement was the main source of reduction in candidate land, while conservation-designated land accounted for most of the excluded stable-core area

These results show that conventional future-suitability maps can overestimate the reliability of long-term cultivation opportunities when they do not distinguish among suitability, climate stability, and land-use feasibility. The mapped climate-stable cultivation refugia, defined here as baseline S1 areas retained as S1 in at least 8 of 10 GCM–scenario projections, should be interpreted as uncertainty-aware decision-support priorities rather than empirically verified demographic refugia. Their overlap with protected land highlights the need to reconcile medicinal plant development with biodiversity conservation through site-specific assessments of forest classification, land tenure, approved management plans, and permissible land-use practices.

The workflow may be adapted to other climate-sensitive medicinal plants and mountain crops, but its ecological thresholds, Fuzzy-AHP weights, veto criteria, class breakpoints, and land-use rules must be locally recalibrated and independently validated. The main limitations are the use of literature-derived occurrence records, the multi-temporal baseline and coarse effective information resolution of climatic inputs, static non-climatic predictors, and sensitivity of stable-core boundaries to predictor specification. Priority next steps are field surveys of high-consensus zones, evaluation of local microclimate and cultivation performance, verification of legal and land-tenure conditions, and integration of socioeconomic feasibility into site-level planning.

Data and Code availability

The datasets generated and analysis code supporting this study, including scripts for data preprocessing, ecological suitability modeling, future climate analysis, model–scenario consensus analysis, climate-stable

refugia identification, and land-use considerations assessment, are available in the Zenodo repository at https://doi.org/10.5281/zenodo.20678258.

Data Source

The climatic, topographic, soil, and land-cover datasets analyzed in this study are all publicly available from their providers: CHELSA v2.1 (https://chelsa-climate.org), the CHELSA-CMIP6 projections, the 30 m SRTM (https://earthexplorer.usgs.gov), SoilGrids 2.0 (https://soilgrids.org), and ESA WorldCover 2021 v200 (https://esa-worldcover.org). The presence records were compiled from published literature on P. notoginseng in Vietnam; their provenance, coordinate type, and positional quality are documented in Supplementary Table S15. No records were retrieved from GBIF, and no primary field survey was undertaken for this study.

Funding Declaration

This work was supported by Tay Bac University under grant number TTB2024-44 (approximately USD 1,140).

Competing interests

The authors declare no competing interests.

Author contributions

Both authors contributed to the conception and design of the study. T.A.P. (Tay Bac University) compiled the datasets, performed the spatial analysis, and drafted the manuscript. T.A.P. (KTH Royal Institute of Technology and Ton Duc Thang University) contributed to the methodological design, supervised the analysis, and revised the manuscript. Both authors read and approved the final version.

Declaration of use of AI tools

An AI-based language tool (Claude, Anthropic) was used solely for language editing of the manuscript text. The authors rechecked and refined it to ensure the language was correct and appropriate. All data processing, analysis, and figures (including Figure 1, which was drawn by the authors in general-purpose diagramming software) are the authors' own, and the authors take full responsibility for the content and conclusions of the work.

References

1. Nguyen, M. H. Chemical constituents and diverse pharmacological effects of Panax notoginseng. *DTU Journal of Science and Technology* **74**, 4–11 (2026).

2. Mancuso, C. Panax notoginseng: Pharmacological Aspects and Toxicological Issues. *Nutrients* **16**, 2120 (2024). https://doi.org/10.3390/nu16132120

3. Li, W., Shi, H. & Wu, X. A narrative review of Panax notoginseng: Unique saponins and their pharmacological activities. *J. Ginseng Res.* **49**, 118–133 (2025). https://doi.org/10.1016/j.jgr.2024.12.005

4. Mu, R. *et al.* Synergistic effects of ginsenoside Rb1 and peroxiredoxin 6 in enhancing myocardial injury treatment through anti-inflammatory, anti-oxidative, and anti-apoptotic mechanisms. *J. Ginseng Res.* **49**, 145–155 (2025). https://doi.org/10.1016/j.jgr.2024.11.003

5. Tran, T. M. A., Eitzinger, J. & Duong, A. Q. Land suitability classifications in response to ecological requirements of Panax notoginseng in Vietnam. *J. Agrometeorol.* **27**, 377–380 (2025). https://doi.org/10.54386/jam.v27i3.3013

6. IPCC. *Climate Change 2021 – The Physical Science Basis*. (Cambridge University Press, 2023). https://doi.org/10.1017/9781009157896

7. Lenoir, J. & Svenning, J. C. Climate-related range shifts - a global multidimensional synthesis and new research directions. *Ecography* **38**, 15–28 (2015). https://doi.org/10.1111/ecog.00967

8. Rana, S. K. *et al.* Climate-change threats to distribution, habitats, sustainability and conservation of highly traded medicinal and aromatic plants in Nepal. *Ecol. Indic.* **115**, 106435 (2020). https://doi.org/10.1016/j.ecolind.2020.106435

9. Kumar, D., Singh, M. & Sharma, S. Fate of important medicinal plants in the eastern himalaya in changing climate scenarios: A case of Panax pseudoginseng Wall. *Appl. Ecol. Environ. Res.* **17**, 13493–13511 (2019). http://dx.doi.org/10.15666/aeer/1706_1349313511

10. Zhang, H., Cui, X., Zhang, Y., Wang, Z. & Liu, Z. Global warming-driven changes in the suitable habitat of ostryopsis davidiana (Betulaceae) Shrubs. *Sustainability* **17**, 6332 (2025). https://doi.org/10.3390/su17146332

11. Akinci, H., Özalp, A. Y. & Turgut, B. Agricultural land use suitability analysis using GIS and AHP technique. *Comput. Electron. Agric.* **97**, 71–82 (2013). https://doi.org/10.1016/j.compag.2013.07.006

12. AbdelRahman, M. A. E., Yossif, T. M. H. & Metwaly, M. M. Enhancing land suitability assessment through integration of AHP and GIS-based for efficient agricultural planning in arid regions. *Sci. Rep.* **15**, 31370 (2025). https://doi.org/10.1038/s41598-025-14051-7

13. Uyan, M., Janus, J. & Ertunç, E. Land use suitability model for grapevine (Vitis vinifera L.) cultivation using the best worst method: A case study from Ankara/Türkiye. *Agriculture* **13**, 1722 (2023). https://doi.org/10.3390/agriculture13091722

14. Pilevar, A. R., Matinfar, H. R., Sohrabi, A. & Sarmadian, F. Integrated fuzzy, AHP and GIS techniques for land suitability assessment in semi-arid regions for wheat and maize farming. *Ecol. Indic.* **110**, 105887 (2020). https://doi.org/10.1016/j.ecolind.2019.105887

15. O'Neill, B. C. *et al.* The Scenario Model Intercomparison Project (ScenarioMIP) for CMIP6. *Geosci. Model Dev.* **9**, 3461–3482 (2016). https://doi.org/10.5194/gmd-9-3461-2016

16. Eyring, V. *et al.* Overview of the Coupled Model Intercomparison Project Phase 6 (CMIP6) experimental design and organization. *Geosci. Model Dev.* **9**, 1937–1958 (2016). https://doi.org/10.5194/gmd-9-1937-2016

17. Brun, P., Zimmermann, N. E., Hari, C., Pellissier, L. & Karger, D. N. Global climate-related predictors at kilometer resolution for the past and future. *Earth Syst. Sci. Data* **14**, 5573–5603 (2022). https://doi.org/10.5194/essd-14-5573-2022

18. Farr, T. G. *et al.* The shuttle radar topography mission. *Rev. Geophys.* **45**, RG2004 (2007). https://doi.org/10.1029/2005RG000183

19. Poggio, L. *et al.* SoilGrids 2.0: Producing soil information for the globe with quantified spatial uncertainty. *SOIL* **7**, 217–240 (2021). https://doi.org/10.5194/soil-7-217-2021

20. FAO. *A Framework for Land Evaluation*. (Food and Agriculture Organization of the United Nations, 1976).

21. Tan, Y. *et al.* Comparison of AHP and BWM methods based on ArcGIS for ecological suitability assessment of Panax notoginseng in Yunnan Province, China. *Ind. Crops Prod.* **199**, 116737 (2023). https://doi.org/10.1016/j.indcrop.2023.116737

22. Zhan, P. *et al.* Assessment of suitable cultivation region for Panax notoginseng under different climatic conditions using MaxEnt model and high-performance liquid chromatography in China. *Ind. Crops Prod.* **176**, 114416 (2022). https://doi.org/10.1016/j.indcrop.2021.114416

23. Guo, Y. *et al.* Prediction of Chinese suitable habitats of Panax notoginseng under climate change based on MaxEnt and chemometric methods. *Sci. Rep.* **14**, 16434 (2024). https://doi.org/10.1038/s41598-024-67178-4

24. van Vuuren, D. P. *et al.* The representative concentration pathways: An overview. *Clim. Change* **109**, 5–31 (2011). https://doi.org/10.1007/s10584-011-0148-z

25. Riahi, K. *et al.* The Shared Socioeconomic Pathways and their energy, land use, and greenhouse gas emissions implications: An overview. *Glob. Environ. Change* **42**, 153–168 (2017). https://doi.org/10.1016/j.gloenvcha.2016.05.009

26. Tebaldi, C. *et al.* Climate model projections from the Scenario Model Intercomparison Project (ScenarioMIP) of CMIP6. *Earth Syst. Dyn.* **12**, 253–293 (2021). https://doi.org/10.5194/esd-12-253-2021

27. Liu, C., Zuo, Z., Xu, F. & Wang, Y. Study of the suitable climate factors and geographical origins traceability of Panax notoginseng based on correlation analysis and spectral images combined with machine learning. *Front. Plant Sci.* **13**, 1009727 (2023). https://doi.org/10.3389/fpls.2022.1009727

28. Zheng, Y. et al. Suitable soil moisture contents for water use efficiency and saponins accumulation in Panax notoginseng. *Chin. Herb. Med.* **13**, 267–273 (2021). https://doi.org/10.1016/j.chmed.2020.10.002

29. Li, P., Zuo, Z. & Wang, Y. Research on the synergistic prediction of the suitable distribution and chemical components of Panax Notoginseng under the background of climate warming. *BMC Plant Biol.* **25**, 1115 (2025). https://doi.org/10.1186/s12870-025-07169-3

30. Urban, M. C. Escalator to extinction. *Proc. Natl. Acad. Sci. U. S. A.* **115**, 11871–11873 (2018). https://doi.org/10.1073/pnas.1817416115

31. Araújo, M. B. & New, M. Ensemble forecasting of species distributions. *Trends Ecol. Evol.* **22**, 42–47 (2007). https://doi.org/10.1016/j.tree.2006.09.010

32. Esen, F., Karadeniz, E., Sunbul, F., Adigüzel, A. D. & Sajjad, M. From mapping to decision making: a hybrid rule-based and machine learning framework for spatial land-use zoning. *Front. Environ. Sci.* **14**, 1791582 (2026). https://doi.org/10.3389/fenvs.2026.1791582

33. Adiguzel, F., Karadeniz, E., Emir, T., Arslan, F. & Ozel, H. B. Balancing conservation and development through explainable machine learning and NSGA-II: a case study of Osmaniye. *Land* **15**, 881 (2026). https://doi.org/10.3390/land15050881

34. Hirzel, A. H., Le Lay, G., Helfer, V., Randin, C. & Guisan, A. Evaluating the ability of habitat suitability models to predict species presences. *Ecol. Modell.* **199**, 142–152 (2006). https://doi.org/10.1016/j.ecolmodel.2006.05.017

35. O'Brien, R. M. A caution regarding rules of thumb for variance inflation factors. *Qual. Quant.* **41**, 673–690 (2007). https://doi.org/10.1007/s11135-006-9018-6

36. National Assembly of the Socialist Republic of Vietnam. *Law on Forestry No. 16/2017/QH14*, adopted November 15, 2017; effective January 1, 2019. Hanoi, Vietnam: National Assembly; 2017.

Supplementary Files

This is a list of supplementary files associated with this preprint. Click to download.

- RV2.Supplementary17092026.docx